QUADRUPOLAR $S_1(J)$ + $S_0(J)$- AND HEXADECAPOLAR U- TRANSITIONS IN H_2 AT 77 K INDUCED BY INTERMOLECULAR COLLISIONS

AMARJIT SEN

QUADRUPOLAR $S_1(J) + S_0(J)$- AND HEXADECAPOLAR U-TRANSITIONS IN H_2 AT 77 K INDUCED BY INTERMOLECULAR COLLISIONS

by

Amarjit Sen

A thesis submitted in partial fulfillment
of the requirements for the degree of
Master of Science

Department of Physics
Memorial University of Newfoundland

December 1978

St. John's Newfoundland
Canada

CONTENTS

ABSTRACT

Double transitions $S_1(J) + S_0(J)$ corresponding to the vibration-rotation transition in one molecule and a rotational transition in the other molecule, occurring simultaneously in a colliding pair, have been observed in the infrared fundamental band of normal H_2 at 77 K for gas densities in the range 100 - 320 amagat with a 2 m absorption cell. These transitions arise because of the contribution to the intermolecular interaction by the anisotropic component of the polarizability of one molecule in the quadrupole field of the other and occur in the high-wavenumber tail of the $S_1(J)$ and $Q_1(J) + S_0(J)$ components of the band. The experimental profiles were analyzed by assuming appropriate line-shape functions and using the available matrix elements of the quadrupole moment, isotropic polarizability and anisotropy of the polarizability of the H_2 molecule. From this analysis the characteristic half-width parameter δ_q and the binary and ternary absorption coefficients of the $S_1(J) + S_0(J)$ transitions have been obtained.

U-branch transitions corresponding to $\Delta J = +4$ in the fundamental band of normal H_2 at 77 K for gas densities up to 520 amagat have also been investigated. These transitions arise on account of the hexadecapolar induction

mechanism in the colliding pairs of molecules and occur on the high-wavenumber wing of the $S_1(1) + S_0(1)$ transition. Although a preliminary report on the observation of the U-transitions was made by previous researchers, no analysis of the profiles was attempted prior to the present work. We have now carried out the profile analysis of these transitions by assuming a line shape similar to that of the quadrupolar lines of the band and using the recently available matrix elements of the hexadecapole moment of the H_2 molecule. The characteristic half-width parameter δ_u and the binary and ternary absorption coefficients of the U branch transitions have been obtained from the analysis.

ACKNOWLEDGMENTS

I wish to thank my supervisor, Professor S.P. Reddy for his helpful suggestions and assistance during this research project.

I express my gratitude to Dr. R.D.G. Prasad who rendered all possible help during the absence of my supervisor who was on sabbatical leave for one year.

I am specially indebted to Dr. J.C. Lewis for his assistance in computer-programming, numerous discussions and encouragement at all stages of the work.

It is my pleasure to acknowledge the help received from the technical services of the Department of Physics and also the other members of the Department.

I take this opportunity to thank the Memorial University of Newfoundland, St. John's, Newfoundland, Canada, for the award of a Graduate Fellowship.

Finally, I wish to extend my grateful thanks to the State Government of Orissa for granting me leave of absence from the Department of Education and Youth Services, and the Government of India for permission to do research abroad.

CHAPTER 1

INTRODUCTION

Because of the $D_{\infty h}$ point group symmetry, homonuclear diatomic molecules such as hydrogen have no electric dipole moment in their ground electronic state and consequently these molecules are normally infrared-inactive. However, an induced and transient dipole moment can occur in these nonpolar molecules by intermolecular interactions during binary or higher order collisions. The induced dipole moment is modulated by the rotation and vibration of the colliding molecules and by their relative translational motion. The molecules thus absorb energy from the radiation-field through the interaction of the induced dipole moment with the field, and hence vibration-rotation (in the fundamental and overtone regions), pure rotation and translation spectra result. Pure translational absorption occurs in the far infrared whereas rotation and vibration-rotation absorption occur at relatively higher wavenumber regions.

The collision-induced fundamental infrared absorption band of H_2 was first observed by Welsh, Crawford and Locke (1949) soon after their discovery of the phenomenon of collision-induced absorption in compressed O_2 and N_2 and since has been studied by different investigators

under various experimental conditions. A comprehensive review of the work done on this topic until 1971 is given by Welsh (1972) and for subsequent work the reader is referred to Reddy et al. (1977) and Gibbs et al. (1974) and the references therein.

In general, the electric dipole moment (μ) in a pair of homonuclear diatomic molecules induced during a collision depends on the internuclear separation of each molecule, the intermolecular separation (R) between their centers of gravity and the relative orientation of each molecule with respect to R. In the so-called 'exponential -4' model of Van Kranendonk (1957 and 1958) the induced dipole moment is expressed as the sum of two additive moments: a short-range isotropic moment with $\mu_{overlap} \propto \exp(-R)$ and a long range angle-dependent (quadrupole-induced) moment with $\mu_{quad} \propto R^{-4}$. The first part, which arises due to the distortion of the electron charge-distribution of the colliding pair at close encounter, gives rise mainly to the broad $Q_{overlap}(\Delta J=0)$ transitions. The second part which results from the polarization of one molecule in the quadrupole-field of the other, gives rise to the relatively less broad $O(\Delta J=-2)$, $Q_{quad}(\Delta J=0)$ and $S(\Delta J=+2)$ transitions, J being the rotational quantum number. Throughout this thesis subscripts 0 and 1 are attached to the transitions O, Q, S and U, etc., to designate the change in the vibrational quantum number v, i.e., 0 for pure rotational band

and 1 for fundamental band.

The collision-induced absorption, also known as pressure-induced absorption for phenomenological reasons, is very much density-dependent. The integrated absorption coefficient of a band which is the area under a band-profile varies almost quadratically with gas density up to moderate pressures. These spectra are rather quite broad (typically several hundred cm^{-1} or more) which is due to the very short-lived dipole moment. At low temperature the bands narrow down substantially. Because of the Maxwellian velocity-distribution, the interaction of the relative translational motion of the colliding molecules with their rotation and vibration gives a characteristic asymmetry to the shape of the absorption bands. At moderate pressures a dip occurs in the Q region which is due to the intercollisional interference effect of the induced dipoles in successive collisions. The dip is strictly density-dependent.

A common feature of collision-induced spectra is the occurrence of double transitions in which both the molecules of a collision pair simultaneously absorb a single quantum of radiation. These are of special importance in the study of a pure gas. In the quadrupole-induction mechanism, the isotropic part of the polarizability of a colliding molecule contributes to the intensity of the single transitions $O_1(J)$, $Q_1(J)$ $(J\neq 0)$ and $S_1(J)$, and the double transitions of the form $Q_1(J) + Q_0(J)$ $(J\neq 0$ for the orientational

transition) and $Q_1(J) + S_0(J)$; on the other hand, the anisotropic component of the polarizability contributes to the intensity of the double transitions of the form $S_1(J) \pm S_0(J)$. Pure rotational double transitions $S_0(J) + S_0(J)$ of H_2 have been observed experimentally by Kiss and Welsh (1959). An indication of the absorption feature corresponding to $S_1(0) + S_0(0)$ in the profile of fundamental band of para hydrogen at 20 K has been reported by Watanabe and Welsh (1967), but no detailed study of the double transitions $S_1(J) + S_0(J)$ of gaseous H_2 has yet been reported prior to the present work (see Chapter 3).

The next higher non-vanishing multipole of a hydrogen molecule after quadrupole is hexadecapole. In the 'exponential-4' model discussed above the hexadecapolar interaction was not considered. As a matter of fact, an induced dipole moment results from the polarization of a molecule by the hexadecapole field of its collision partner with $\mu_{hexa} \propto R^{-6}$ and it gives rise to the selection rule $\Delta J = 0, \pm 2$ and ± 4. But such transitions are expected to be relatively weak because of the small magnitude of the hexadecapole moment. The discovery of the hexadecapole-induced U transitions ($\Delta J=+4$) of the form $U_1(J)$ and $Q_1(J) + U_0(J)$ in the fundamental band of H_2 in the gaseous phase at 195 K has recently been reported by Gibbs et al. (1974) and in the solid phase at 10 K by Prasad et al. (1978). Some preliminary observation of these U transitions

in normal H_2 at 77 K has been reported by Chang (1974). For the first time a profile analysis of the U-transitions has been attempted in this work (see Chapter 4).

In the collision-induced fundamental band of normal H_2 at 77 K all possible transitions arising from the induction mechanisms discussed earlier are shown in Fig. 1. At this temperature almost all the molecules are distributed among the rotational levels J = 0 and 1 of the ground vibrational state. The energy levels in Fig. 1 are calculated from the constants of the free H_2 molecule (Foltz et al., 1966) and the transitions are shown in the following six groups: (i) $Q_1(J)$; (ii) $S_1(0)$ and $Q_1(J) + S_0(0)$; (iii) $S_1(1)$ and $Q_1(J) + S_0(1)$; (iv) $S_1(J) + S_0(J)$; (v) $U_1(0)$ and $Q_1(J) + U_0(0)$; and (vi) $U_1(1)$ and $Q_1(J) + U_0(1)$. Double transitions $Q_1(J) + Q_0(1)$ involving only an orientational transition are not shown in the figure. Extensive work has been done on the former three groups of transitions by previous workers. The objective of the present work is to make a systematic study of the latter three groups.

Recently, the collision-induced fundamental band of normal hydrogen at 77, 196 and 298 K has been studied in great detail by Reddy et al. (1977) for gas densities up to 60 amagat with 1 m and 2 m absorption cells. A typical profile with analysed components at 77 K by these authors is reproduced in Fig. 2. Altogether, 11 components (two overlap and nine quadrupolar) of significant intensity

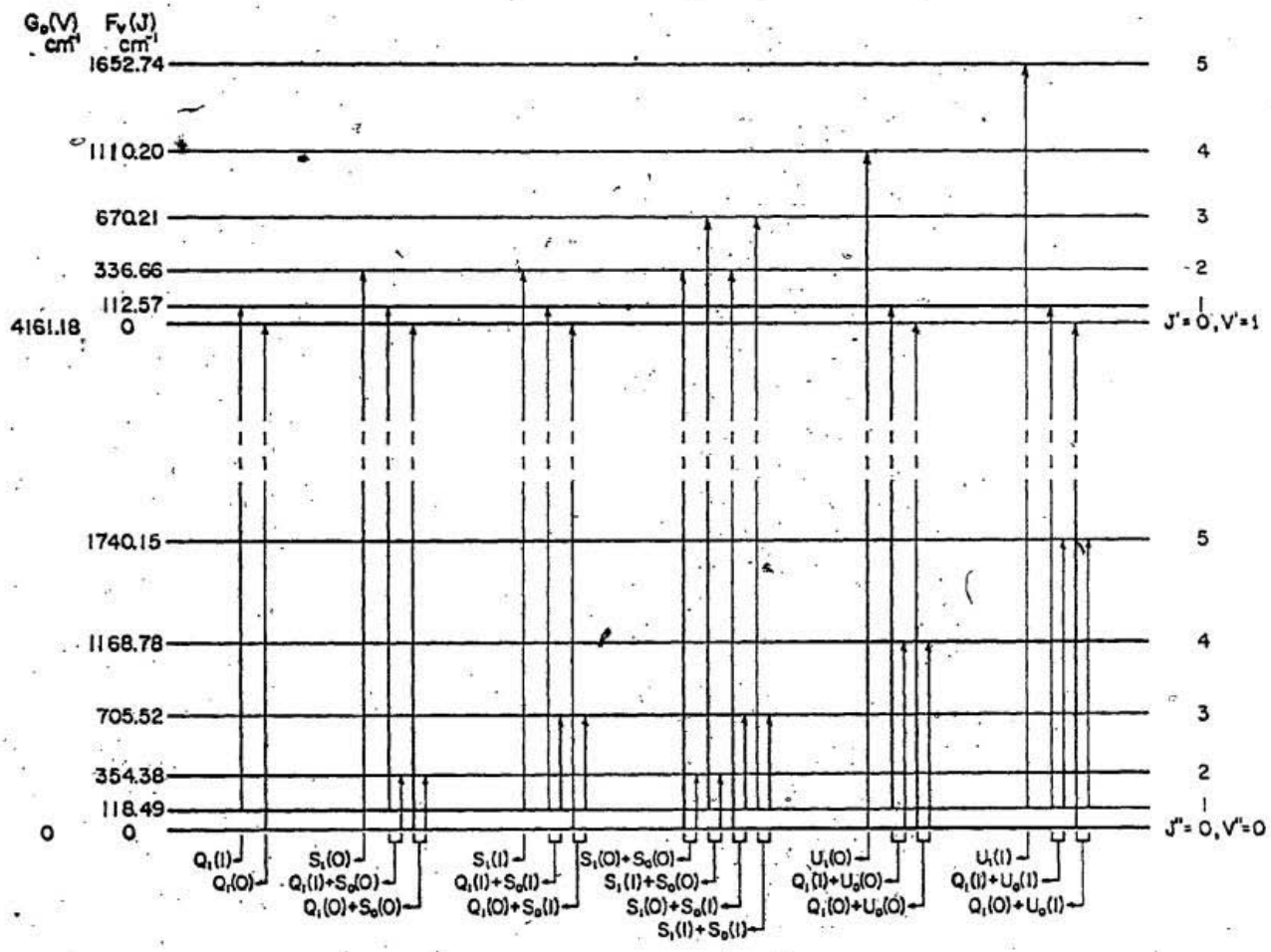

Fig. 1. Energy level diagram showing transitions arising from different induction mechanisms in the collision-induced fundamental band of normal H_2 at 77 K (see text for details).

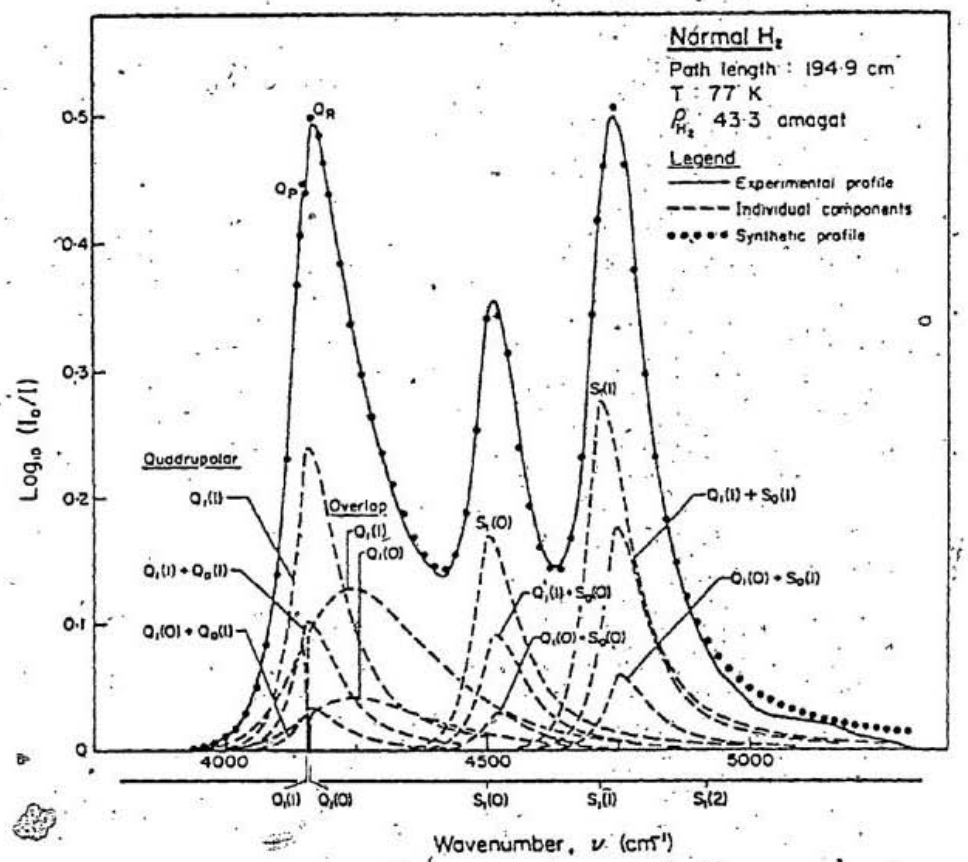

Fig. 2. An Absorption profile of the collision-induced fundamental band of normal H_2 at 77 K at a gas density of 43.3 amagat. The solid curve is the experimental profile. Two overlap-induced and nine quadrupole-induced components are represented by dashed curves and the summation of these is represented by dots. (Ref. Reddy et al. 1977).

are shown in the figure.

Analysis of the experimental absorption profiles of the fundamental band of H_2 in the pure gas has been done by several researchers (Chisholm and Welsh, 1954; Kiss and Welsh, 1959; Hunt and Welsh, 1964; Watanabe and Welsh, 1967; Watanabe, 1971; and Reddy et al., 1977). In the recent work of Reddy et al. (1977), the so-called Levine-Birnbaum line-shape (Levine and Birnbaum, 1967) in the form of a modified Bessel function of the second kind for the intracollisional part and a dispersion-type line-shape for the intercollisional part* (Van Kranendonk, 1968) have been used for the analysis of the overlap-induced Q components. Further, in the same work of Reddy et al., an empirical dispersion-type line shape (Kiss and Welsh, 1959) has been used for the quadrupolar components. The relative intensities of the latter have been calculated from the theoretical values of the matrix elements of the quadrupole moment and polarizability of the hydrogen molecule obtained by Birnbaum and Poll (1969) and Poll (1971), respectively (see Chapter 3 for details).

The double transitions of the form $S_1(J) + S_0(J)$ arising from the anisotropy of the polarizability are not noticeable in the profiles of the fundamental band of H_2, obtained in the density range up to 60 amagat of the gas at 77 K with the 2 m absorption cell (see Fig. 2). But in the present work when the density of the gas is

*Also see Lewis (1976) and the references therein for a detailed theoretical treatment of intercollisional interference.

increased beyond 100 amagat up to ~320 amagat these transitions appear with significant intensity. The experimental profiles, their detailed analysis and the binary and ternary absorption coefficients for these transitions are presented in Chapter 3.

When the density of the gas in the absorption cell at 77 K is further increased in the range 300 to 520 amagat, the hexadecapole-induced U-transitions are observed with measurable intensity on the high wavenumber wing of the overlap and the quadrupolar transitions. In order to separate the weak U-transitions in the spectral region of interest from the relatively strong wing of the overlap and quadrupolar transitions, an empirical expression for the entire wing and a dispersion-type line-shape for the U-transitions were used. The analysis and the results of this phase of the work are presented in Chapter 4.

A description of the experimental set up and details of the technique are given in Chapter 2.

CHAPTER 2

INSTRUMENTS AND TECHNIQUE

The present research project on some new aspects of collision-induced infrared absorption of molecular hydrogen in the fundamental band, whose objectives have been outlined in Chapter 1, was carried out at 77 K with a low-temperature high-pressure absorption cell and an infrared spectrometer. A brief description of the apparatus used and an account of the experimental procedure adopted will be presented in this chapter.

2.1. The 2 m Absorption Cell

The 2 m transmission-type absorption cell, originally designed by Reddy and Kuo (1971) for room-temperature work and later used in a modified form for low-temperature work by Chang (1974) and Prasad (1976) has been used in the present work.

The cell constructed from a 2 m stainless steel bar has a central bore of 1 in. and a 1 in. thick wall. A highly polished light-guide assembled linearly from five individual sections has a rectangular aperture 1 cm x 0.5 cm and was fitted coaxially in the cell. The light-guide not only serves as a transmitter of radiation from one end to

the other by multiple reflections, but also reduces the volume inside the cell. At each end of the cell there was an optically flat synthetic sapphire window 1 cm thick and 2.54 cm in diameter, which was attached by means of General Electric RTV-108 silicone rubber cement to a polished stainless steel window-seat having an aperture 0.4 in. x 0.2 in. The design provided an appropriate mechanism for a pressure-tight seal between the window-seat and the body of the cell by means of an invar O-ring.

To prevent the windows from frosting during low-temperature work each end of the cell was provided with a small cylindrical vacuum chamber which consisted of a stainless steel tube and a plexiglas adapter. A flat sapphire window 5.08 cm in diameter and 3 mm thick was appropriately sealed to the latter for transmission of infrared radiation. The plexiglas adapter was kept warmer by passing a small current (~ 0.2 amp) through a heating coil wound around it. The two vacuum chambers were under constant evacuation during the experiments.

The cell was housed in a double-walled cylindrical stainless steel jacket and held in it by suitable supporting discs. The inner cavity of the jacket was insulated with vermiculite. Provision was made in the design to accommodate the contraction occurring in the inner cylinder of the jacket when the cell was cooled. Liquid coolants could

be poured into the jacket through an opening provided at the top and the cell was kept submerged in it. Liquid nitrogen (77 K) was used as the coolant in the present experiments.

A steel capillary tube joined to the middle of the cell by means of a 0.5 in. Aminco fitting was connected to the gas-handling system for gas inlet. The sample path-lengths of the cell are 195.3 cm at 298 K and 194.9 cm at 77 K. For more constructional details the reader is referred to Prasad (1976).

2.2. The Infrared Monochromator and Optical System

The arrangement of the source of continuous infrared radiation and the focusing optics with respect to the 2 m absorption cell and the monochromator is shown schematically in Fig. 3. The source is a 600 watt General Electric FFJ Quartzline projection lamp operated approximately at 75 volts and 4 amps by a stabilized power-supply unit. The lamp was housed in a water-cooled brass jacket of a special design (see Chang, 1974, for details). Radiation from the source was focused on the entrance window of the cell by a front-coated concave mirror having a radius of curvature of 60 cm and an aperture of 15 cm. Radiation coming out from the exit window of the cell was focused by a similar mirror on to the entrance slit (S_1) of a Perkin-Elmer Model 99 single-beam double-pass monochromator equipped with a lithium

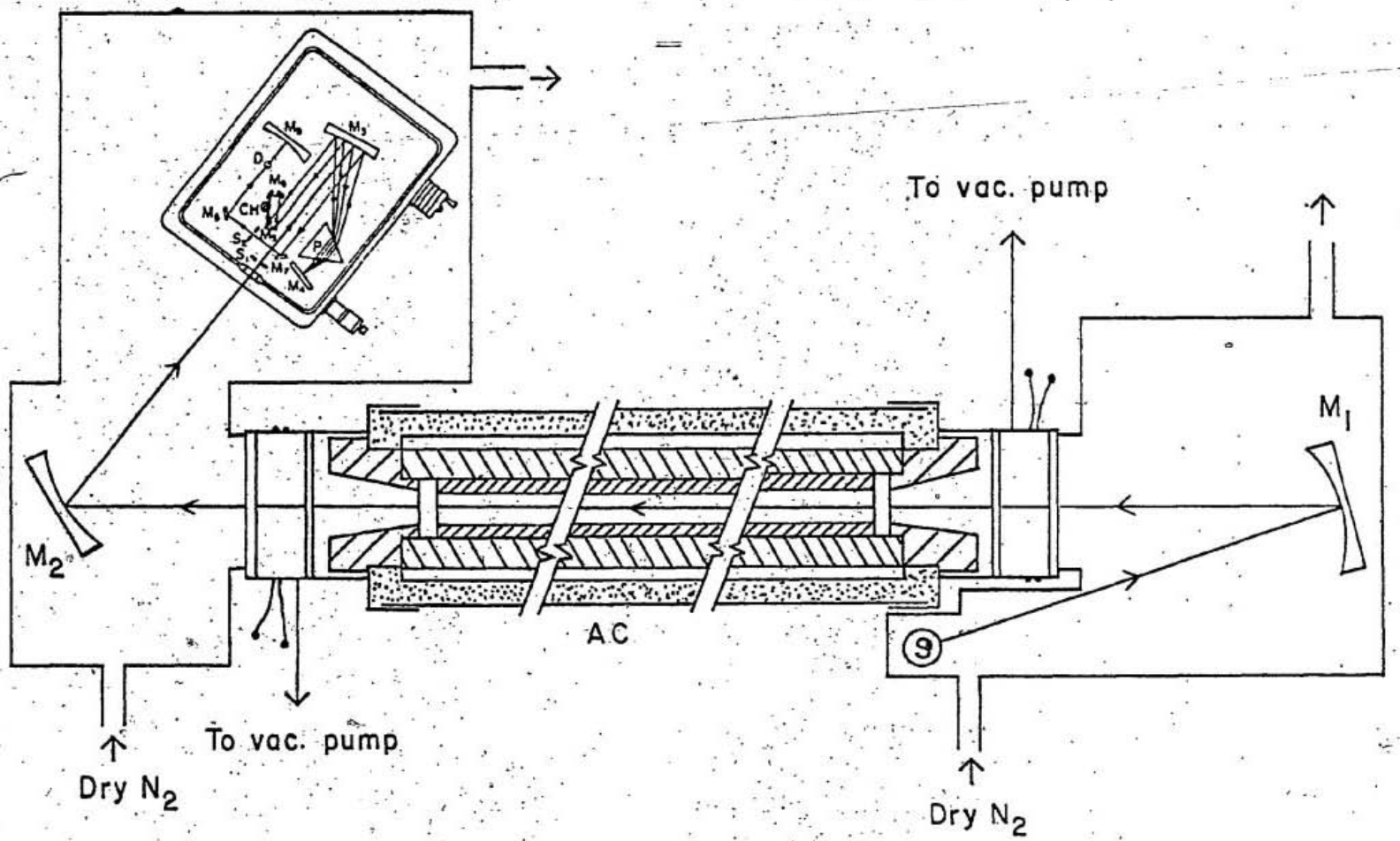

Fig. 3. A cross-sectional view of the absorption cell and the optical arrangement: S: source, M_1, M_2, and M_9: spherical mirrors, AC : absorption cell, S_1 and S_2: entrance and exit slits, M_3: a 21° off-axis parabolic mirror, M_4: littrow mirror, M_5-M_8: plane mirrors, CH: tuning fork chopper, D: PbS detector.

fluoride prism (P) and an uncooled lead sulphide detector (D). The optical path of a monochromatic radiation is shown schematically in Fig. 3. Radiation after the first pass through the prism and reflection from the littrow mirror (M_4) was brought to a focus between the plane mirror (M_6) and the tuning fork chopper (CH) (American Time Products Model L-40) by a 21° off-axis parabolic mirror (M_3). The diverging beam from this focus was chopped at a frequency of 260 Hz by the chopper. The pulsating beam was dispersed by the prism and reflected by the littrow mirror and brought first to a focus on to the exit slit (S_2) and then to a final focus on to the detector.

The littrow mirror was coupled to a wavenumber drum which could be rotated by a three-speed motor-drive, thus making it possible to scan a spectral region of interest at the desired speed. The slit width was maintained at 35 μm which gave spectral resolutions of ~3·5 cm^{-1} at 4161 cm^{-1} (origin of the fundamental band of H_2) and ~5.0 cm^{-1} at 5000 cm^{-1}.

2.3. The Detection-Amplification-Recording System

In general, a semiconductor detector such as PbS has a quicker response to a signal than a conventional thermal detector such as a thermocouple, bolometer or a golay pneumatic detector. In the present case the radiation chopped at a frequency of 260 Hz was focused on the element

of the uncooled PbS detector which converted it into an a.c. signal. A schematic diagram of the detection-amplification-recording system used in the present work is shown in Fig. 4. The signal was first amplified by a pre-amplifier (Brower Laboratories Model 261) and then fed into a lock-in voltmeter (Brower Laboratories Model 131) together with a square-wave reference signal from the chopper. In the lock-in voltmeter the d.c. base of the signal was filtered out while the signal itself and the noise were amplified and then fed into a push-pull transformer and a relay contact. The reference signal was suitably phase-matched and fed to the same relay system. The positive half-cycles of the two signals were mixed in such a way that a full wave rectified d.c. output resulted. Any ripple in this output was filtered out by an RC filter-unit and the resulting output was fed to a strip chart recorder (Leeds and Northrup Model S60 000 type G) which recorded the spectrum continuously.

2.4. The Gas-handling System

The gas-handling system is schematically shown in Fig. 5. The absorption cell was connected to a Matheson 'ultra-high-pure' hydrogen cylinder by stainless steel Aminco fittings and through a liquid nitrogen trap C made of a copper coil 0·25 in. in outer diameter. The Bourdon tube pressure-gauges G_1, G_2 and G_3 were calibrated against standard oil gauges which in turn were calibrated against an Ashcroft dead-weight pressure-balance. The maximum pressures

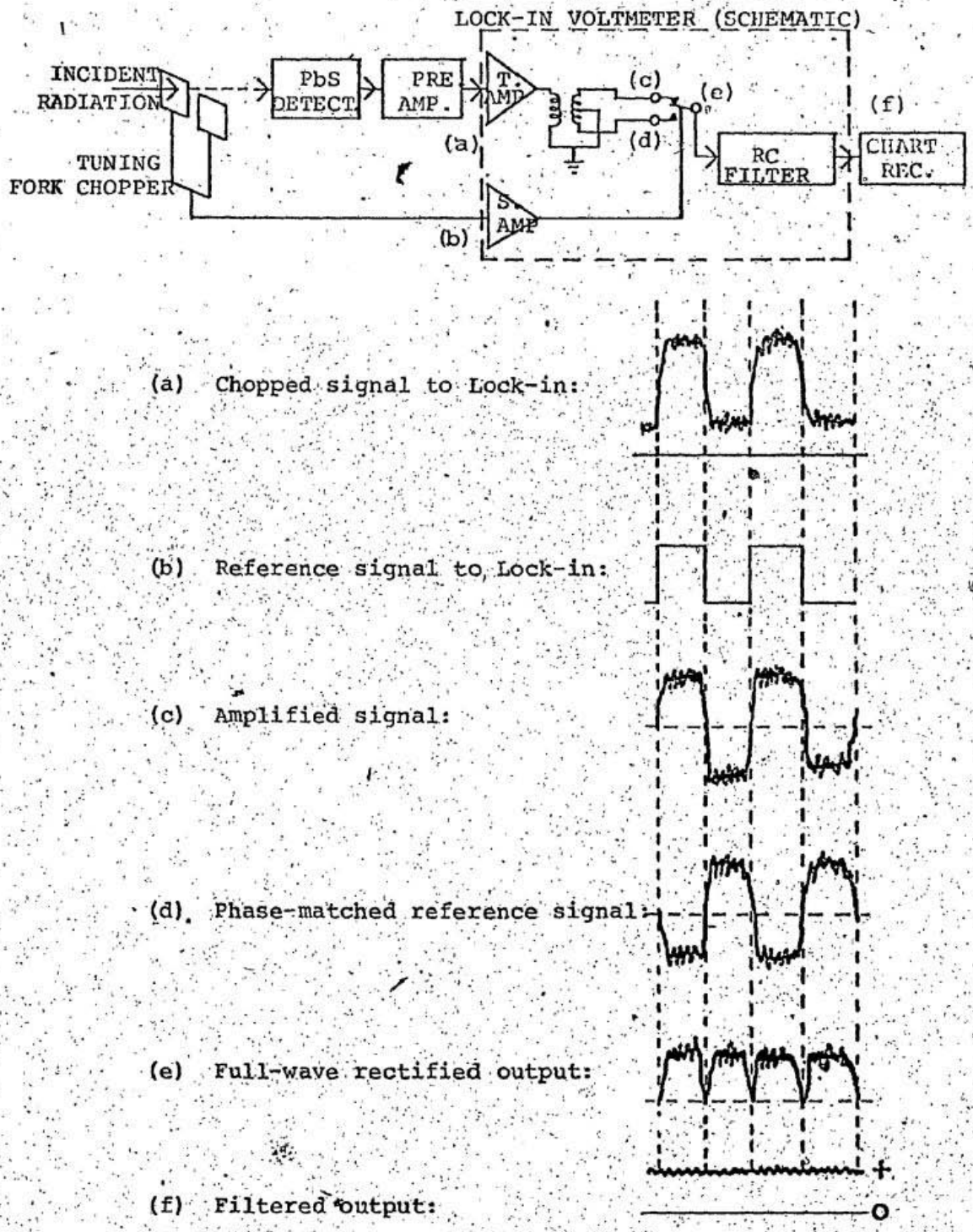

Fig. 4. Block diagram of the signal detection - amplification - recorder system with a tuning fork chopper. Also shown schematically is the signal behavior at various stages in the circuit.

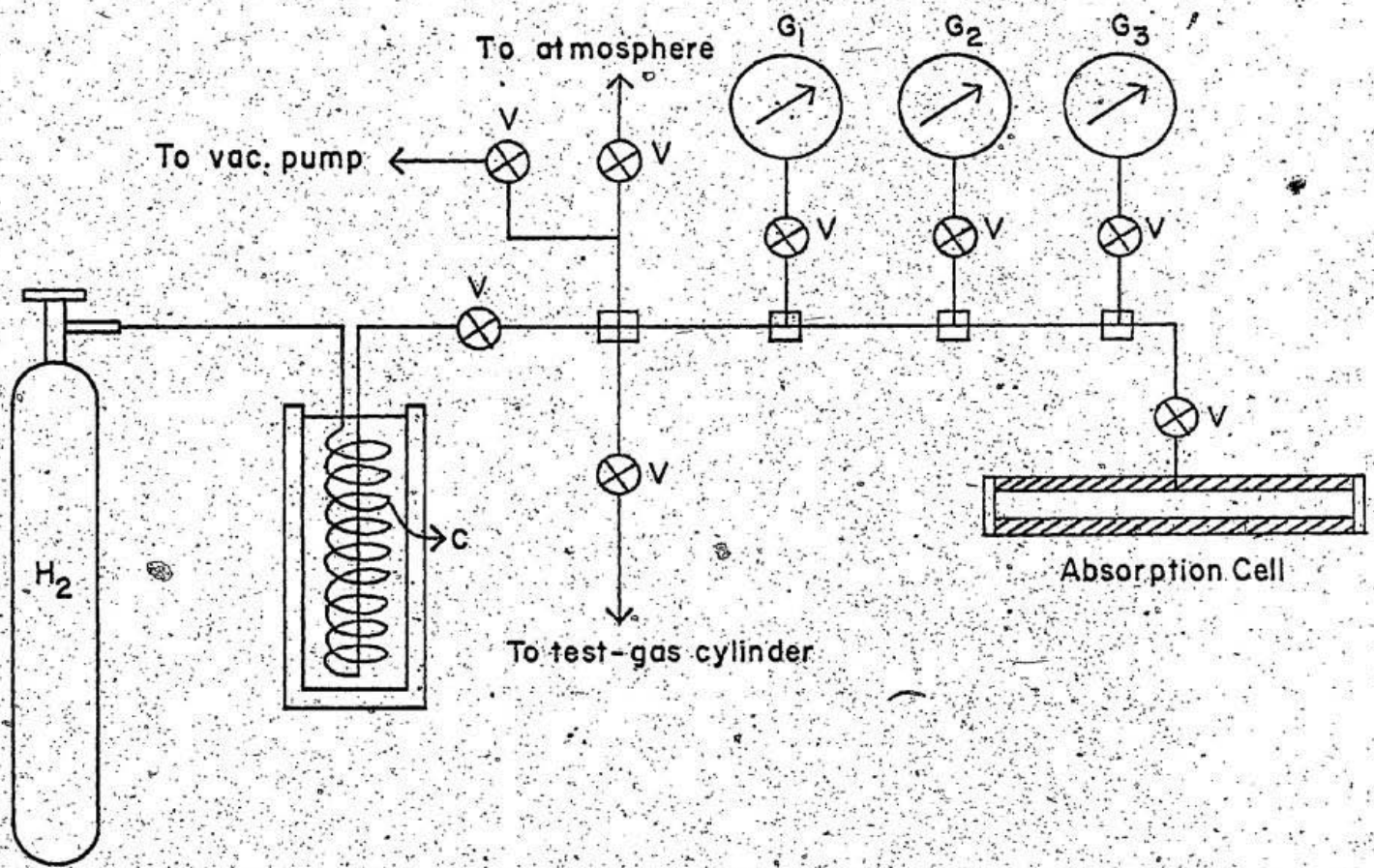

Fig. 5. The gas-handling system.

that can be read on the gauges are 500, 1000 and 5000 p.s.i., respectively. All the valves in the system are Aminco high-pressure needle valves. The copper coil (C) was used as a thermal compressor and the required pressures in the experiments were generated by admitting H_2 gas into it when it was immersed in liquid N_2 and then allowing it to reach room temperature. Before an experiment was performed, the entire gas-handling system including the cell was tested for good vacuum and for pressures higher than the experimental ones.

2.5. Removal of Water Vapor from the Optical Path

Since the strong atmospheric water vapor absorption peaks around 1.8 μm and 2.6 μm interfere with the spectral region of interest in the present study, it was necessary to remove the atmospheric water vapor from the optical path of the infrared radiation for reliable absorption measurements. This was achieved by keeping the whole optical path except the absorption cell in an atmosphere of nitrogen gas which has no detectable absorption in this spectral region.

Two air-tight plexiglas boxes, one housing the source and a concave mirror and the other the monochromator and a second concave mirror were connected to the ends of the cell by rubber hoses (see Fig. 3). Each box was provided with an inlet and an outlet for the nitrogen gas. The outlets were fitted with one-way-flow valves so that

atmospheric air could not get into the boxes in the reverse way. Two neoprene gloves were fitted to the two opposite sides of the box containing the monochromator for handling the monochromator without breaking the air-tight seal. The boxes were continuously flushed with dry nitrogen gas boiled off from a dewar containing liquid nitrogen by passing a small current through a 10 watt resistor immersed in it. The flow of nitrogen into the boxes was regulated by the amount of current in the resistor. Initially it took nearly two weeks to reduce the water vapor level to a satisfactory minimum. Experiments were conducted when this minimum remained steady.

2.6. Calibration of Spectral Region and Reduction of Recorder Traces of Spectra

Mercury emission lines (Humphreys, 1953; Plyler et al., 1955; and Zaidal et al., 1970), atmospheric water vapor absorption peaks (Downie, 1953; Plyler, 1952 and 1960, and IUPAC Tables of Wavenumbers 1977) and neon emission lines (Rao et al., 1966) were used as standards for calibration of the spectral region 3500 - 6500 cm^{-1}. The distances of the emission and absorption peaks were measured accurately from the Hg-emission-line at 6535.95 cm^{-1}. A least squares polynomial fit of these distances of the spectral lines against their wavenumbers was made by trying out several degrees of the polynomial with an IBM 370 computer. The coefficients obtained from the best fit were used for

drawing the calibration chart at intervals of 5 cm^{-1} in the region 3500 - 6500 cm^{-1} with the help of a CALCOMP plotter on a PDP 12 computer. The positions of two standard Hg-lines and that of a water vapor absorption peak were used as references on the calibration chart.

The absorption coefficient $\alpha(\nu)$ at a given wavenumber $\nu(cm^{-1})$ of hydrogen at a density ρ_{H_2} in a cell of sample length ℓ is given by $(1/\ell)\ln[I_0(\nu)/I(\nu)]$, where $I_0(\nu)$ and $I(\nu)$ are the intensities of radiation transmitted by the evacuated cell and by the cell filled with hydrogen, respectively. The wavenumber calibration chart was superimposed on the recorder traces with the help of standard reference lines and the quantity $\log_{10}[I_0(\nu)/I(\nu)]$ was measured at intervals of 5 cm^{-1} by using a standard logarithmic scale. Absorption profiles were obtained by plotting $\log_{10}[I_0(\nu)/I(\nu)]$ against wavenumber ν. The integrated absorption coefficient of a specific branch of a band or of a band itself, i.e., $\int\alpha(\nu)d\nu$, was obtained from the area under the absorption profile.

2.7. Isothermal Data for Hydrogen at 77 K

In the studies of collision-induced absorption the density of a gas is usually expressed in units of amagat which is the ratio of the density of the gas at the experimental conditions to its density at STP. The density of the gas expressed in amagat when multiplied by Loschmidt's number gives directly the number of molecules in a cm^3 of

volume. The pressure-density data of hydrogen at 77 K for pressures up to 100 atm were obtained from Dean (1961) and for higher pressures from Goodwin et al. (1963).

CHAPTER 3

ABSORPTION PROFILES OF THE $S_1(J) + S_0(J)$ TRANSITIONS IN NORMAL H_2 AT 77 K AND THEIR ANALYSIS

The possibility of the occurrence of the double transitions $S_1(J) + S_0(J)$ in the fundamental band of H_2 involving $\Delta J = +2$ in each of the molecules of a colliding pair, which arise from the anisotropy of their polarizability has been outlined in Chapter 1. In the present work the absorption spectra of these transitions at 77 K have been recorded for gas densities in the range 100 - 320 amagat with a 2 m cell. At this temperature only four transitions of this group arising from J = 0 and 1 are of importance (see Fig. 1). The contribution of the individual transitions of the group to the intensity of the observed spectra was separated by a method of profile analysis. In this chapter we present the details of the experimental profiles of these transitions, their analysis and the information obtained on the characteristic half-widths and the absorption coefficients. Experimental details and the method of obtaining the absorption profiles have been described in Chapter 2.

3.1. The Absorption Profiles

Figure 6 shows three absorption profiles of the collision-induced fundamental band of normal H_2 in the pure gas at 77 K for the densities 150, 227 and 321 amagat in the spectral region 4800 - 6000 cm^{-1}. The positions of the four principal double transitions $S_1(J) + S_0(J)$ with $J = 0$ and 1, calculated from the constants of the free H_2 molecule (Foltz et al., 1966), are marked along the wavenumber axis. These transitions were not noticeable at 77 K in the density range up to 60 amagat with a 2 m cell (Reddy et al.; see for example Fig. 2). For the range of densities above ~100 amagat, the absorption due to the Q and the main S branches in the spectral region below ~4800 cm^{-1} became so large that it went beyond the infinity absorption line on the recorder charts and a distinct peak appeared at ~5300 cm^{-1} with another noticeable feature at ~5075 cm^{-1}. In Fig. 6 this distinct peak at ~5300 cm^{-1} corresponds to $S_1(1) + S_0(1)$ (calculated wavenumber: 5299.9 cm^{-1}) and the second absorption peak at ~5075 cm^{-1} corresponds to $S_1(1) + S_0(0)$ and $S_1(0) + S_0(1)$ transitions (calculated wavenumbers: 5067.3 and 5084.8 cm^{-1}, respectively). The absorption-peak corresponding to $S_1(0) + S_0(0)$ (4852.2 cm^{-1}) which is masked by the other strong components is not obvious in this figure. With the increase in pressure a small absorption peak around 5750 cm^{-1}, indicated by a * in this figure is observed, which corresponds to the

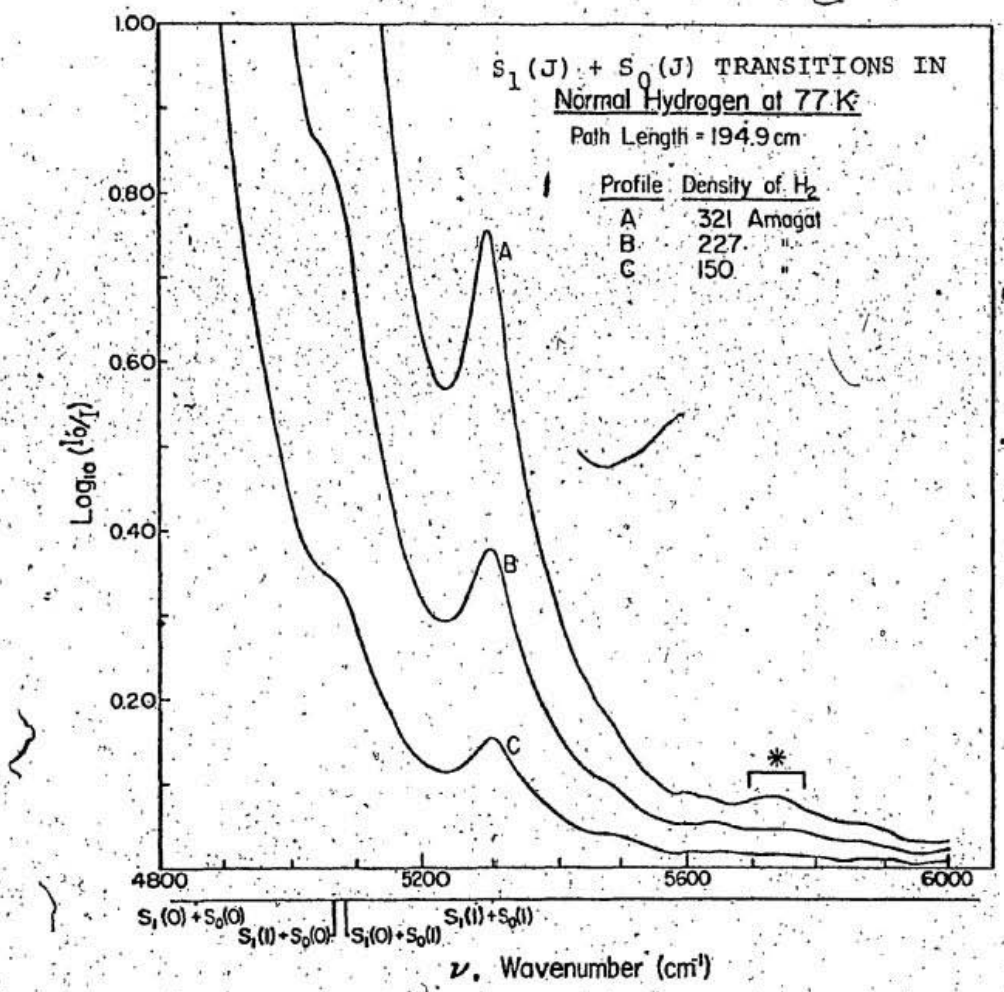

Fig. 6. Absorption profiles of the collision-induced fundamental band of normal H_2 in the pure gas at 77 K for different densities in the spectral region 4800 - 6000 cm^{-1} where the double transitions $S_1(J) + S_0(J)$ with J=0 and 1 appear predominantly.

hexadecapolar U transitions to be discussed in the next chapter.

3.2. The Profile Analysis

When the absorption cell contains a large amount of H_2, the high wavenumber wings of the strong components of its fundamental band, namely, $Q_1(J)$ (overlap and quadrupolar), $S_1(J)$ and $Q_1(J) + S_0(J)$, contribute considerably to the intensity of the band in the spectral region of the comparatively weak double transitions $S_1(J) + S_0(J)$. In order to obtain the intensity and other information about these weaker transitions, the contribution of the wings of the stronger components superimposing the former is separated by a method of profile analysis which is described in the following paragraphs.

(a) The Absorption Coefficient and Line Shapes

The absorption coefficient $\alpha(\nu)$ at a given wavenumber ν of the fundamental band is represented by a summation of the contributions of all the individual transitions in the form (Van Kranendonk, 1968; see also Mactaggart and Welsh, 1973, and Reddy et al., 1977)

$$\alpha(\nu) = \sum_{m,n} \left\{ \frac{\tilde{a}^0_{nm}\nu}{1 + \exp(-hc\Delta\nu/kT)} \right\} W_n(\Delta\nu) . \qquad (3\text{-}1)$$

Here, n represents the type of induction mechanism (0 for overlap induction, 1 for quadrupolar induction with

isotropic polarizability, 2 for quadrupolar induction with anisotropic polarizability, 3 for hexadecapolar induction, etc.), m denotes a particular transition in a given mechanism, $\tilde{\alpha}^0_{nm}$ is a parameter representing the maximum absorption coefficient (which is a fictitious one for the overlap components) at the molecular wavenumber ν_m, $W_n(\Delta\nu)$ with $\Delta\nu = \nu - \nu_m$ represents the line-shape function of the n-type mechanism, h, c and k are the fundamental constants and T is the absolute temperature.

It has been shown by Poll (1960) that the transitions due to a particular type of induction mechanism have the same line shape. In Eq. (3-1) the factor in the denominator on the right converts the symmetrized line-form into the observed asymmetric line-form. A detailed discussion of the line shapes is given by Mactaggart and Welsh (1973) and Reddy et al., (1977).

In Eq. (3-1) the line-shape function for the overlap transitions is given by the expression (note n = 0 in this case)

$$W_0(\Delta\nu) = W_0^0(\Delta\nu)\ D(\Delta\nu), \qquad (3\text{-}2)$$

where

$$W_0^0(\Delta\nu) = (2\Delta\nu/\delta_d)^2\ K_2(2\Delta\nu/\delta_d) \qquad (3\text{-}3)$$

is the Levine-Birnbaum (1967) expression (which has some theoretical basis), K_2 being the modified Bessel function of the second kind and δ_d being the intracollisional

half-width at half height. The quantity $D(\Delta\nu)$ is the Van Kranendonk's (1968) expression for the intercollisional part with δ_c defined as the intercollisional half-width at half height and is expressed as

$$D(\Delta\nu) = 1 - \gamma[1 + (\Delta\nu/\delta_c)^2]^{-1} , \qquad (3-4)$$

where γ is a constant, usually chosen as unity to make the intensity of the dip at the molecular wavenumber go to zero. The dips in the overlap components of the fundamental band of H_2 can be seen in Fig. 2.

The empirical line-shape function of the quadrupolar transitions (used so far for the components arising from the isotropic polarizability) is a dispersion-type function which is represented by (note n = 1).

$$W_1(\Delta\nu) = 1/\{1 + (\Delta\nu/\delta_q)^2\} , \qquad (3-5)$$

where δ_q is the quadrupolar half-width at half-height. As the double transitions $S_1(J) + S_0(J)$ originate basically from the quadrupolar induction mechanism, the same line-shape and the same half-width will be assumed for these transitions in the present work.

(b) The Relative Intensities

According to Van Kranendonk (1958) the relative intensity of the mth component of the overlap-induced transitions i.e., $Q_{1\ \text{overlap}}(J)$, is given by

$$\bar{\alpha}^0_{0m} \propto P_J , \qquad (3-6)$$

where P_J is the normalized Boltzmann factor (i.e., $\Sigma_J P_J = 1$) for the rotational level J, and is given by

$$P_J = \frac{g_T(2J+1)\exp(-E_J/kT)}{\Sigma_J g_T(2J+1)\exp(-E_J/kT)} \quad . \qquad (3\text{-}7)$$

In the above relation g_T is the nuclear statistical weight factor for the rotational states (g_T = 1 and 3 for the even and odd J states, respectively) and E_J is the rotational energy of the Jth level of H_2 calculated from its rotational constants (Foltz et al., 1966). Equation (3-7) is true for equilibrium hydrogen. For normal hydrogen $\Sigma_{J,odd} P_J / \Sigma_{J,even} P_J = 3/1$. The relative intensities of the overlap transitions were expressed in terms of the intensity of the strongest of them, i.e., that of Q_1 overlap(1).

The relative intensity of the mth quadrupolar transition arising from isotropic polarizability (i.e., for Q_{quad}, S, Q+Q and Q+S transitions) is given by (Poll, 1971)

$$\tilde{\alpha}^0_{1m} \propto \sum_{J_1,J_2} P_{J_1} P_{J_2} [C(J_1 2J_1';00)^2 \langle v_1'J_1'|Q_1|0J_1\rangle^2 \, C(J_2 0J_2';00)^2 \langle v_2'J_2'|\alpha|0J_2\rangle^2$$

$$+ C(J_1 0J_1';00)^2 \langle v_1'J_1'|\alpha_1|0J_1\rangle^2 \; C(J_2 2J_2';00)^2 \langle v_2'J_2'|Q_2|0J_2\rangle^2] \; , \qquad (3\text{-}9)$$

where the subscripts 1 and 2 refer to the two colliding molecules, $C(J\lambda J';00)$ with λ = 0 and 2 are the Clebsch-Gordan coefficients, $\langle|\alpha|\rangle$'s are the matrix elements of the polarizability α obtained from Poll (1971), and $\langle|Q|\rangle$'s are the matrix elements of the quadrupole moment Q obtained

from Poll and Wolniewicz (1978), of the H_2 molecule. It is to be noted that for the fundamental band of H_2, $v_1' = 1$ and $v_2' = 0$ or vice versa. The relative intensities of the transitions in this group are expressed in terms of that of $S_1(1)$.

For the double transitions $S_1(J) + S_0(J)$ arising from the anisotropy (γ) of the polarizability, the relative intensity of the m th transition is given by (McKellar and Welsh, 1971)

$$\bar{\alpha}^0_{2m} \propto \sum_{J_1,J_2} P_{J_1} P_{J_2} [C(J_1 2 J_1'; 00)^2 C(J_2 2 J_2'; 00)^2 \times$$

$$\{ \frac{2}{9} (\langle v_1' J_1' | Q_1 | 0 J_1 \rangle^2 \langle v_2' J_2' | \gamma_2 | 0 J_2 \rangle^2 + \langle v_1' J_1' | \gamma_1 | 0 J_1 \rangle^2 \langle v_2' J_2' | Q_2 | 0 J_2 \rangle^2)$$

$$- \frac{4}{15} \langle v_1' J_1' | Q_1 | 0 J_1 \rangle \langle v_1' J_1' | \gamma_1 | 0 J_1 \rangle \langle v_2' J_2' | Q_2 | 0 J_2 \rangle \langle v_2' J_2' | \gamma_2 | 0 J_2 \rangle \}], \quad (3\text{-}10)$$

where $\langle | \gamma | \rangle$'s are the matrix elements of the anisotropy of the polarizability obtained from Poll (private communication) and listed in Appendix 1, and the other quantities have the usual meanings as in Eq. (3-9). The relative intensities of these double transitions are expressed in terms of that of $S_1(1) + S_0(1)$.

The relative intensities of all the transitions in the collision-induced fundamental band of H_2 at 77 K are given in Appendix 2.

(c) Method of Computation and Results of Analysis

The primary objective of the profile analysis is to obtain a satisfactory fit between the experimental absorption profile and a synthetic one computed from the functional relation for the absorption coefficient $\alpha(\nu)$ as given by Eq. (3-1) with appropriate line-shape functions for the three different groups of transitions (i.e., n=0, 1 and 2). The maximum intensity factors ($\tilde{\alpha}^0_{0m}$, $\tilde{\alpha}^0_{1m}$ and $\tilde{\alpha}^0_{2m}$ of Q_1 overlap (1), $S_1(1)$ and $S_1(1) + S_0(1)$, respectively) and the half-width δ_q were regarded as adjustable parameters in the computer-program. A shift parameter was also introduced for the molecular wavenumber ν_m to account for any vibrational perturbation effect.

Different initial trial values of the adjustable parameters were used for the computation of the synthetic profile using the experimental data points by a least-squares fit on an IBM 370 computer. In this analysis the values of the half-widths δ_c and δ_d of the overlap components were taken from Reddy et al. (1977). The value of the half-width parameter δ_q was taken from the best fit. A typical example of an analyzed profile in the spectral region 4800 - 6000 cm^{-1} is given in Fig. 7 where the calculated contributions of the wings of the overlap and the quadrupolar (due to isotropic polarizability only) components and those of the individual $S_1(J) + S_0(J)$ transitions with J = 0 and 1 are shown separately. The agreement between the

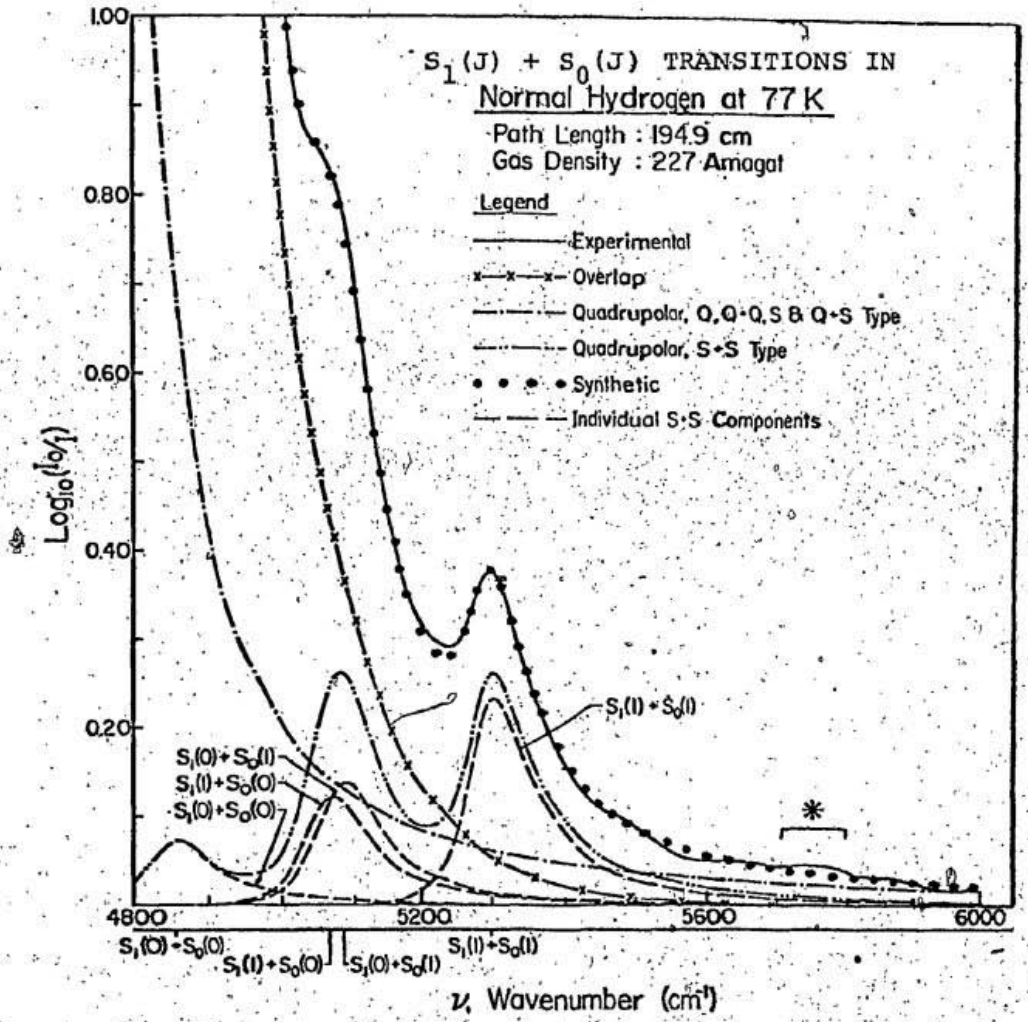

Fig. 7. Analysis of an absorption profile of the fundamental band of normal H_2 in the pure gas at 77K in the region 4800 - 6000 cm^{-1}. The solid curve is the experimental profile. The dots represent the total synthetic profile which is the sum of the dash-x curve representing the overlap-induced wing, the dash-dot curve representing the quadrupole-induced wing due to the isotropic polarizability and the dash-double-dot curve representing total contribution of the quadrupolar $S_1(J) + S_0(J)$ components arising from the anisotropy of the polarizability. The individual $S_1(J) + S_0(J)$ transitions are shown by dashed curves.

experimental and synthetic profiles is very good as seen from the figure. Altogether fifteen absorption profiles were analyzed and the results of the analysis are presented in Table I. The shift-parameter of the molecular wavenumber ν_m for the quadrupolar components seems to be slightly dependent on the density of the gas and has the value -9 ± 2 cm^{-1} in the density range 100 - 320 amagat.

3.3. The Absorption Coefficients of $S_1(1) + S_0(1)$

The integrated absorption coefficients $\int \alpha(\nu) d\nu$ for the transition $S_1(1) + S_0(1)$ for various densities of the H_2 gas were calculated from the areas under the computed profiles (see Fig. 7), which were obtained by numerical integration. The integrated absorption coefficient can be expanded in a power series of the gas density ρ_{H_2} (= ρ_a) as

$$\int \alpha(\nu) d\nu = \alpha_{1a} \rho_a^2 + \alpha_{2a} \rho_a^3 + \ldots , \qquad (3\text{-}11)$$

or

$$\frac{1}{\rho_a^2} \int \alpha(\nu) d\nu = \alpha_{1a} + \alpha_{2a} \rho_a + \ldots , \qquad (3\text{-}12)$$

where α_{1a} and α_{2a} are the binary and ternary absorption coefficients respectively for the transition in question. A plot of the quantity $(1/\rho_{H_2}^2) \int \alpha(\nu) d\nu$ versus ρ_{H_2} is shown in Fig. 8(a) where the intercept and the slope, which gave the binary and ternary absorption coefficients, respectively, were obtained from a linear least-squares fit of the data.

TABLE I. Results of Profile Analysis of nH_2 at 77K.

Intracollisional Half-width	Collision Duration[b]	Quadrupolar Half-width (Symmetrized)	Collision Duration[c]	Molecular Shift of quadrupolar components
δ_d (cm^{-1})	τ_d (10^{-14}s)	δ_q (cm^{-1})	τ_q (10^{-14}s)	S (cm^{-1})
192±5[a]	2.8	54±2	9.83	-9±2

a taken from Reddy et al. (1977)

b $\tau_d = 1/2\pi c\delta_d$

c $\tau_q = 1/2\pi c\delta_q$

TABLE II. Absorption Coefficients of the transition $S_1(1) + S_0(1)$ of H_2 at 77 K

Binary Absorption Coefficient		Ternary Absorption Coefficient
α_{1a}	$\tilde{\alpha}_{1a}$	α_{2a}
(10^{-6} cm^{-2} $amagat^{-2}$)	(10^{-38} cm^6 sec^{-1})	(10^{-9} cm^{-2} $amagat^{-3}$)
6.84±0.21	5.26	7.08±0.98

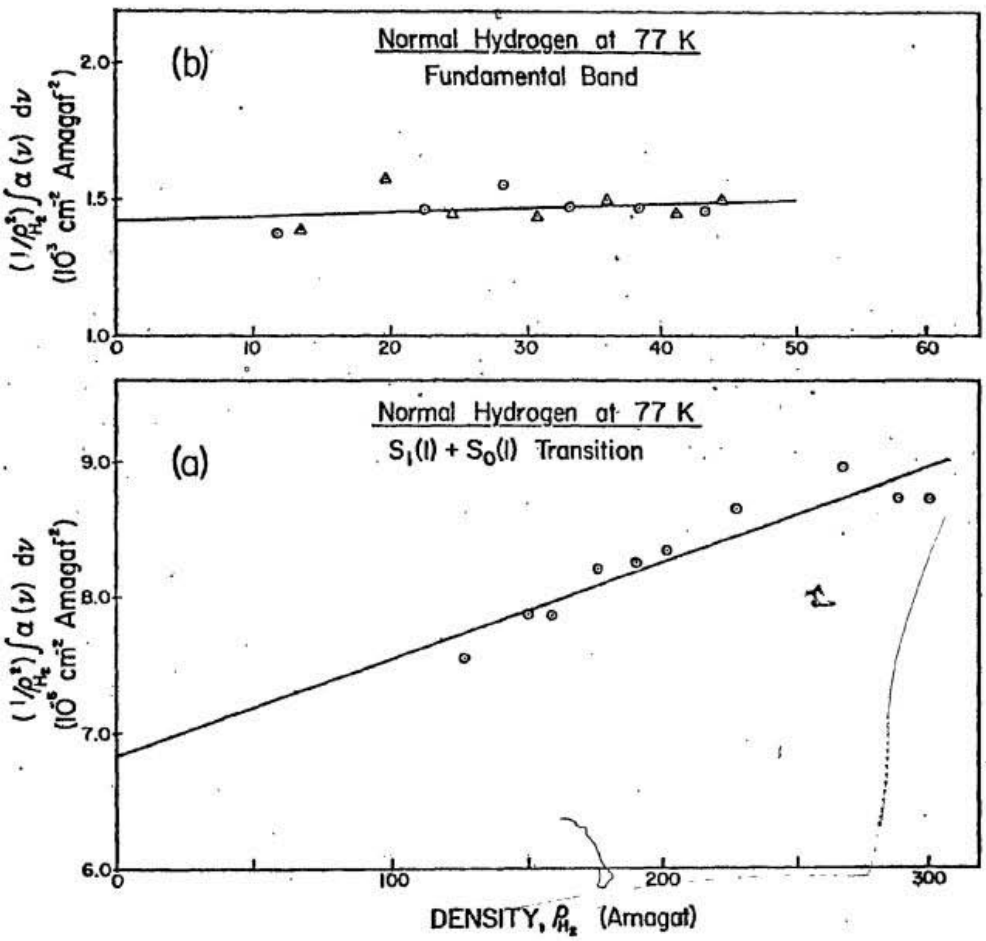

Fig. 8. Plots of $(1/\rho_{H_2}{}^2)\int\alpha(\nu)d\nu$ vs ρ_{H_2} for the profiles of normal H_2 at 77 K for (a) the double transition $S_1(1)$ + $S_0(1)$ for gas densities in the range 125-300 amagat and (b) for the fundamental band as a whole for gas densities up to 60 amagat, taken from Reddy et al. (1977).

A similar plot of the quantities for the fundamental band of normal H_2 at 77 K in the density range up to 60 amagat taken from Reddy et al. (1977) is reproduced in Fig. 8(b) for comparison.

The integrated absorption coefficient can also be represented in the form

$$c\int\tilde{\alpha}(\nu)d\nu = \tilde{\alpha}_{1a}\rho_a^2 n_0^2 + \tilde{\alpha}_{2a}\rho_a^3 n_0^3 + \ldots , \qquad (3\text{-}13)$$

where $\tilde{\alpha}(\nu) = \alpha(\nu)/\nu$ and n_0 is the Loschmidt's number (2.687×10^{19} molecules/cm^3). The new binary and ternary absorption coefficients $\tilde{\alpha}_{1a}$(cm^6 sec^{-1}) and $\tilde{\alpha}_{2a}$(cm^9 sec^{-1}) are related to α_{1a} and α_{2a} by $\tilde{\alpha}_{1a} = (c/n_0^2)\alpha_{1a}/\bar{\nu}$ and $\tilde{\alpha}_{2a} = (c/n_0^3)\alpha_{2a}/\bar{\nu}$ with $\bar{\nu} = \int\alpha(\nu)d\nu/\alpha(\nu)\nu^{-1}d\nu$ as the band center. The value of the band center at 77 K for the $S_1(1) + S_0(1)$ transition is 5395 cm^{-1}.

The values of the binary and ternary absorption coefficients obtained are listed in Table II. The corresponding quantities for the other transitions in this group can be calculated from their relative intensities (see Appendix 2).

3.4. Discussion

As mentioned in Chapter 1, the double transitions in normal H_2 at 77 K involving $\Delta J = +2$ in each of the colliding molecules were not studied in detail in the fundamental band until the present work. These transitions i.e., $S_1(J) + S_0(J)$, are very weak compared to $S_1(1)$, as

can be seen from Fig. 2. However, with increasing gas-density considerable absorption due to these transitions could be recorded.

The experimental value of the binary absorption coefficient i.e., $(\alpha_{1a}/\bar{\nu})$ of the $S_1(1) + S_0(1)$ transition is 1.27×10^{-9} cm^{-1} $amagat^{-2}$ whereas the corresponding theoretical value is 1.28×10^{-9} cm^{-1} $amagat^{-2}$, which are in very good agreement.

The half-width of the quadrupolar transitions at 77 K is found to be 54 ± 2 cm^{-1} which is in excellent agreement with the value obtained previously by Reddy et al. (1977). In the density range 125 - 300 amagat, there seems to be no pressure-narrowing of the quadrupolar lines. The dispersion line-shape fits very well except in the far wing of the profile (see Fig. 7). There is a small departure between the synthetic and experimental profile around 5270 cm^{-1} which may be due to the weak U(0)-group of transitions that lies in that spectral region which has not been taken into account here.

For the best fit of each profile it is found that the molecular wavenumbers of the quadrupolar transitions have to be shifted (on the average by ~ 9 cm^{-1}) toward the low-wavenumber side, which may be due to the perturbation of vibrational levels. Such shifts have already been reported in the binary mixtures of H_2 - X where X is Ar, Kr of Xe (see for example Varghese et al., 1972).

CHAPTER 4

ABSORPTION SPECTRA OF THE U BRANCH ($\Delta J=+4$) TRANSITIONS IN THE FUNDAMENTAL BAND OF NORMAL H_2 AT 77 K

As mentioned in Chapter 1, the U transitions occur in the collision-induced absorption due to the hexadecapolar induction mechanism. Although these transitions in the fundamental band of H_2 in the gas phase were observed earlier, no analysis was reported until the present work. As shown in Fig. 1 (Chapter 1), six U branch transitions, $U_1(J)$ and $Q_1(J) + U_0(J)$ with $J = 0$ and 1 are expected to occur in the fundamental band of normal H_2 at 77 K. In fact all these six transitions have been recently identified in the absorption spectrum of solid H_2 at 10 K by Prasad et al. (1978).

In the present work the absorption due to these U-transitions in the fundamental band of normal H_2 at 77 K has been studied with a 2 m cell for the gas densities in the range 300 - 520 amagat. At these densities the high wavenumber wings of the overlap and quadrupolar transitions have considerable intensity in the main spectral region of the U transitions. We have made an attempt to analyze the band profiles in this region by assuming a new expression

for the contribution of the wings of the overlap and quadrupolar transitions as a whole and a dispersion-type line-shape for the individual components of the U branches. Details of the experimental profiles and their analysis are presented in the following sections of this chapter.

4.1. The Absorption Profiles

As shown in Fig. 6 (Chapter 3) a small absorption feature around ~5750 cm^{-1} (marked with *) appears in the profile at 321 amagat. With further increase in the density of the gas the $S_1(1) + S_0(1)$ transition reaches the infinite absorption line and the peak around 5750 cm^{-1} appears distinctly. Three typical experimental absorption profiles of the collision-induced fundamental band of normal H_2 at 77 K for the gas densities, 437, 473 and 518 amagat in the spectral region 5400 - 6200 cm^{-1} are presented in Fig. 9. The positions of the three transitions of the U(1) group, namely $U_1(1)$ (5695.4 cm^{-1}), $Q_1(1) + U_0(1)$ (5776.9 cm^{-1}) and $Q_1(0) + U_0(1)$ (5782.9 cm^{-1}) calculated from the constants of the free H_2 molecule (Foltz et al., 1966) are shown along the wavenumber axis. The corresponding transitions of the U(0) group which occur in the region ~5300 cm^{-1} are completely masked by the strong wings of the overlap and quadrupolar contributions which reach the infinite absorption line on the recorder chart for the high-density profiles. The absorption peak at ~5750 cm^{-1} in Fig. 9 corresponds to the transition of the U(1) group. All the six transitions

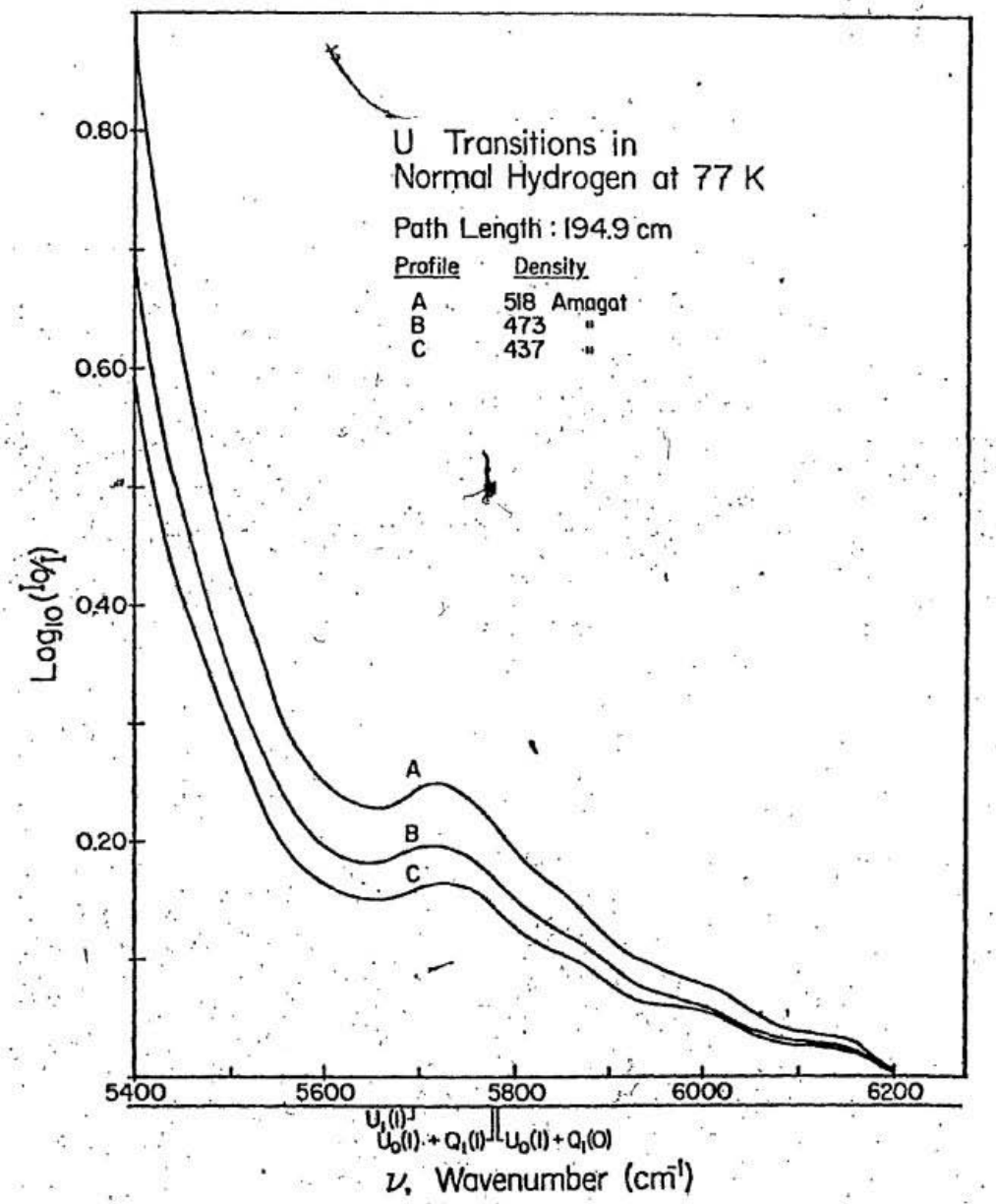

Fig. 9. Absorption Profiles of the Collision-induced fundamental band of normal H_2 at 77 K for three different densities in the range 5400 - 6200cm^{-1}, showing hexadecapolar U-transitions.

of the U(0) and U(1) groups have been taken into consideration in the analysis of band profiles.

4.2. The Profile Analysis

The U-transitions in the fundamental band in the region ~5750 cm^{-1} lie on the predominantly strong high wavenumber tail of the $S_1(1) + S_0(1)$ transition, where the overlap and the other quadrupolar transitions also have considerable contribution. Since the contributions of the overlap and quadrupolar transitions up to ~5400 cm^{-1} (see Fig. 9) almost reach the infinity-absorption-line on the recorder chart, not enough data points are available for trying out a fit with appropriate line-shape functions in this part of the profiles. Therefore the absorption coefficient for the whole of the overlap and quadrupolar parts was expressed by a single functional form (without any half-width parameter). The U transitions, however, were assumed to have a dispersion-type line-shape with a half-width parameter. The actual expressions, the relative intensities of these hexadecapolar transitions and the method of analysis are presented in the following paragraphs.

(a) The Absorption Coefficient and the Line Shape

The total contribution to the absorption coefficient at any wavenumber ν consists of two parts. The part of the absorption coefficient due to the wings of the overlap and quadrupolar contributions in the region of interest where

the tail part of the strong $S_1(1) + S_0(1)$ transition predominates, is represented by (Lewis, private communication)

$$\alpha(\nu) = \frac{a_1^2 \nu}{1 + (\Delta\nu/a_2)^2 + (\Delta\nu/a_3)^4} , \qquad (4\text{-}1)$$

where a_1, a_2 and a_3 are the adjustable parameters and $\Delta\nu = \nu - \nu_s$ with ν_s as the molecular wavenumber of $S_1(1) + S_0(1)$. For the U transitions, Eq. (3-1) used in the analysis of profiles in Chapter 3 was employed with n = 3, and the summation was restricted to the U branch transitions only. An empirical expression of the dispersion form was assumed for the line-shape function $W_3(\Delta\nu)$ for the hexadecapolar transitions which is represented by

$$W_3(\Delta\nu) = \frac{1}{1 + (\Delta\nu/\delta_u)^2} , \qquad (4\text{-}2)$$

where δ_u is the half-width at half height and $\Delta\nu = \nu - \nu_m$ with ν_m as the molecular wavenumber of the m th transition.

(b) The Relative Intensities

The relative intensities of the U transitions (single as well as double) are represented by Karl et al. (1975) as (note n = 3),

$$\tilde{\alpha}^0_{3m} \propto \sum_{J_1 J_2} P_{J_1} C(J_1 4 J_1'; 00)^2 \langle v_1' J_1' | H | v_1 J_1 \rangle^2 P_{J_2} \delta_{J_2 J_2'} \langle v_2' J_2' | \alpha | v_2 J_2 \rangle^2 , \qquad (4\text{-}3)$$

where $C(J_1 4 J_1'; 00)$'s are the Clebsch-Gordan coefficients,

$\langle|H|\rangle$'s are the matrix elements of the hexadecapole moment, $\delta_{JJ'}$ is a Kronecker delta and the other quantities have the same meaning as in Eq. (3-9). The values of the matrix elements $\langle|H|\rangle$ of H_2 are taken from Karl et al. (1975). The relative intensities of the other U-transitions are expressed in terms of that of the $U_1(1)$ transition and are listed in Appendix 2.

(c) The Method of Analysis and Results

A method of analysis similar to the one used in Chapter 3 was followed for the present study and the calculations were performed on a Hewlett Packard 9825A programmable calculator in conjunction with a HP 9871 A Printer and a HP 9862 A X-Y Plotter. A listing of the program is given in Appendix 3. Five different adjustable parameters were used and the value of the hexadecapolar half-width δ_u was obtained from the best fit. A set of ten absorption profiles was analyzed and a typical example of the analysis of an experimental profile with the synthetic profile resulting from the six individual components of the U group is shown in Fig. 10. It is to be noted that the total contribution of $U_1(0)$, $Q_1(1) + U_0(0)$ and $Q_1(0) + U_0(0)$ is shown in this figure. Unlike in the analysis of the profiles of the $S_1(J) + S_0(J)$ transitions, the best fits of the profiles in the U-region were obtained without introducing any shift-parameter for the molecular wavenumber ν_m of the U-transitions.

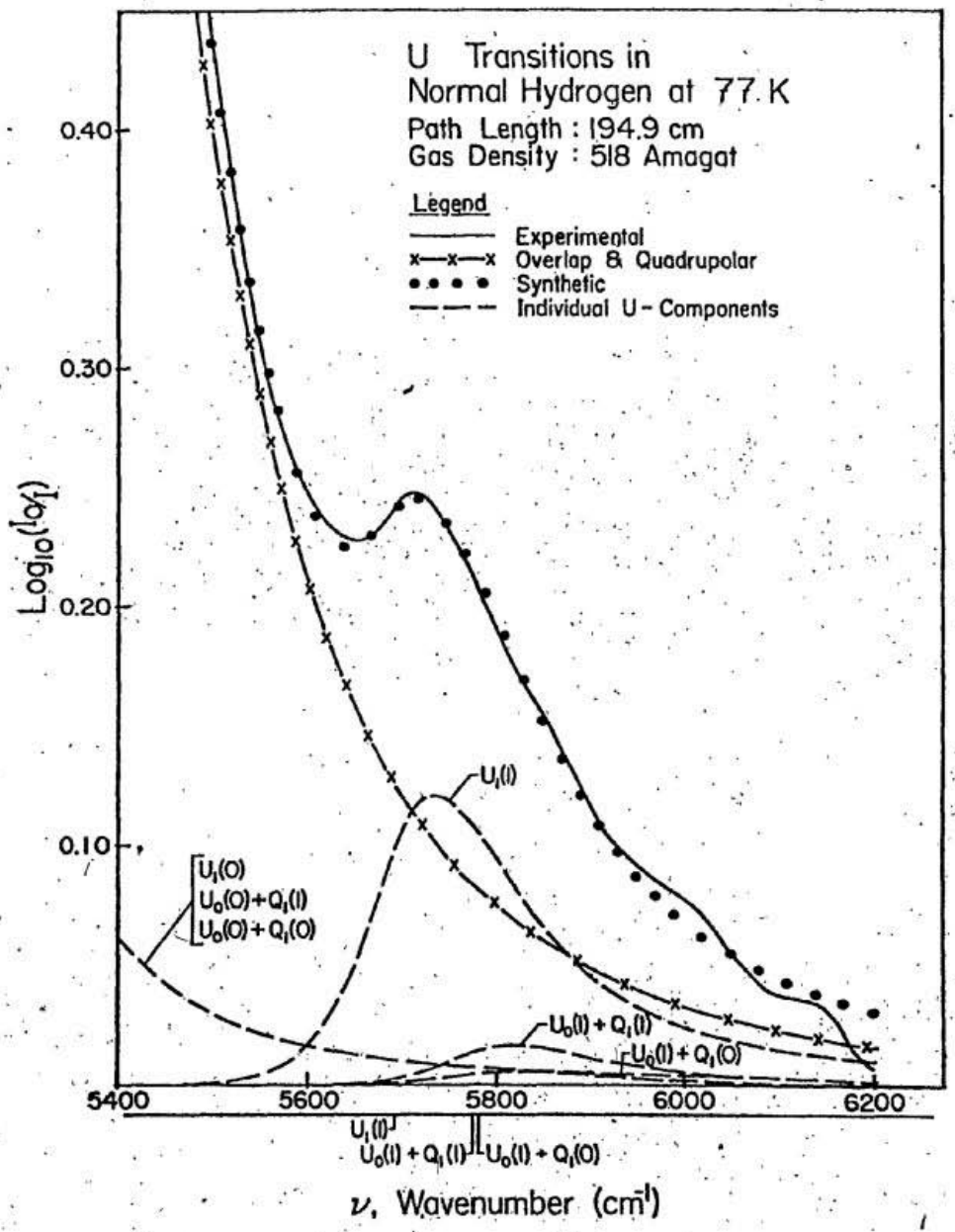

Fig. 10. Analysis of the Absorption Profiles of normal H_2 at 77 K showing individual U-components.

The apparent shift of the $U_1(1)$ peak by about ~40 cm^{-1} towards the high wavenumber side of its molecular frequency is due to the asymmetry of the band profile. As seen from Fig. 10, the agreement between the experimental and synthetic profiles is very good except in the region beyond ~6000 cm^{-1}.

The results of the analysis are given in Table III, in which the half-widths of the overlap (intracollisional) and the quadrupolar components are also included for comparison.

4.3. The Absorption Coefficients of $U_1(1)$

The integrated absorption coefficient $\int\alpha(\nu)d\nu$ of $U_1(1)$ transition in normal H_2 at 77 K is obtained from the computed area under its band-profile. As in Chapter 3, a plot of $(1/\rho_{H_2}^2)\int\alpha(\nu)d\nu$ versus ρ_{H_2} is shown in Fig. 11 and the binary and ternary absorption coefficients obtained in a similar manner, are given in Table IV. The binary absorption coefficients of other components of the U group transitions can be readily obtained from their relative intensities listed in Appendix 2 and the value of the binary absorption coefficient of the $U_1(1)$ transition.

4.4. Discussion

The hexadecapolar U transitions in the normal H_2 at 77 K were analyzed with an empirical line-shape of the dispersion-type and a value of the half-width has been given for the first time. From the dependence of the

TABLE III. Half-widths and collision durations of spectral transitions of H_2 at 77 K arising from different induction-mechanism.

	Induction Mechanism		
	Quadrupolar	Hexadecapolar	Overlap (intracollisional)
Half-width $\delta(cm^{-1})$	54±2	118±8	192±5[a]
Collision duration $\tau(10^{-14}s)$	9.8	4.5	2.8[a]

[a] taken from Reddy et al. (1977).

[b] $\tau = 1/2\pi c\delta$

TABLE IV. Binary and Ternary Absorption Coefficients of the $U_1(1)$ transition of H_2 at 77 K.

Binary Absorption Coefficient		Ternary Absorption Coefficient, α_{2a}
α_{1a}	$\tilde{\alpha}_{1a}$	
$(10^{-6}$ cm^{-2} amagat$^{-2})$	$(10^{-38}$ cm^6 s$^{-1})$	$(10^{-9}$ cm^{-2} amagat$^{-3})$
1.38±0.09	0.98	0.17

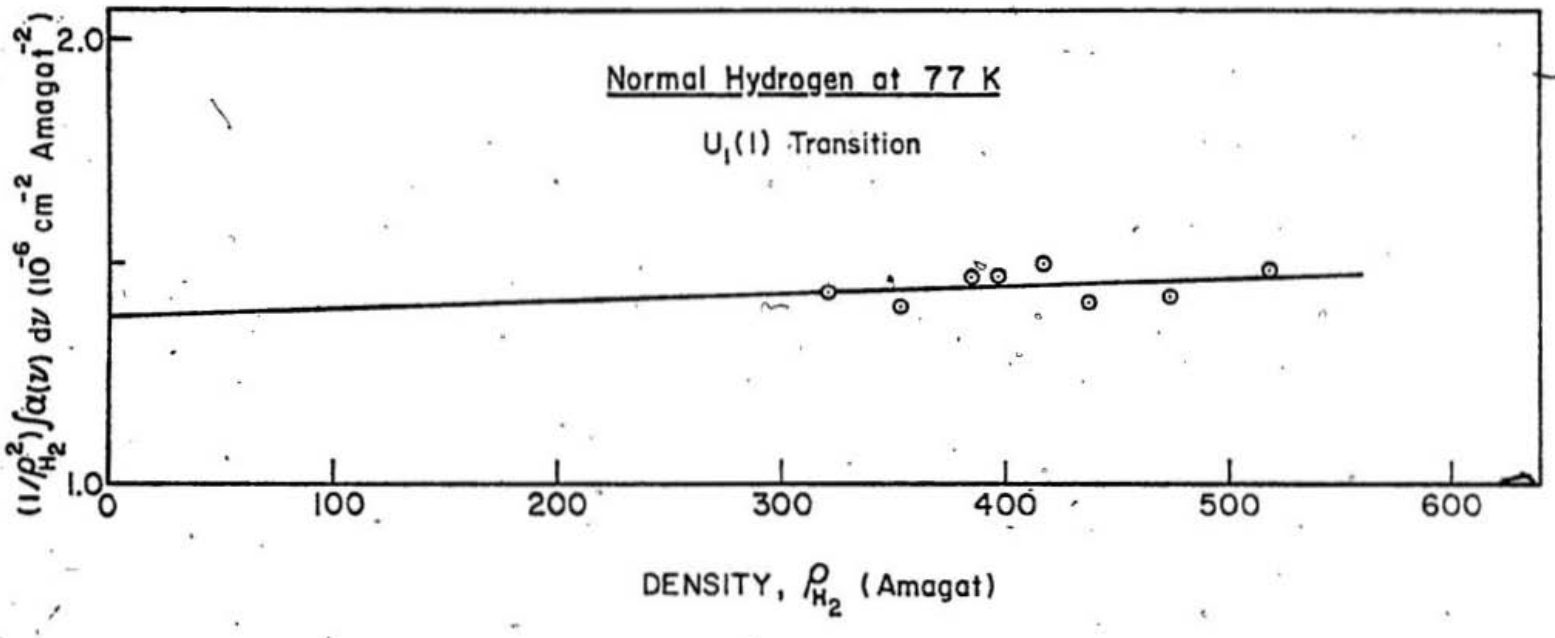

Fig. 11. Plot of $(1/\rho_{H_2}^2)\int\alpha(\nu)d\nu$ vs. ρ_{H_2} for the profiles of normal H_2 at 77 K for $U_1(1)$ transition in the density range 300 - 520 amagat.

induced dipole moment on the intermolecular distance (R) for the three different induction-mechanisms (overlap, quadrupolar, and hexadecapolar) it is expected that the half-width of the hexadecapolar transitions will be somewhere between that of overlap and quadrupolar transitions. A rough theoretical estimate shows that the ratio of the half-widths of hexadecapolar to quadrupolar lines is about 1.7. A comparison of the half-widths of the overlap, quadrupolar and hexadecapolar transitions obtained from experiments shows that the hexadecapolar half-width is about two times and the overlap (intracollisional) half-width is about four times that of the quadrupolar transition (see Table III). The dispersion line-shape seems to fit quite well except at the high wavenumber wing, where the experimental profile falls more rapidly.

The experimental value of the binary absorption coefficient of the $U_1(1)$ transition is 2.36×10^{-10} cm^{-1} $amagat^{-2}$ whereas the theoretical value is 2.66×10^{-10} cm^{-1} $amagat^{-2}$. A comparison of the binary absorption coefficient of the $U_1(1)$ transition with those of $S_1(1) + S_0(1)$ and $S_1(1)$ shows that the former is smaller by factors of 5 and 185, respectively.

It may be appropriate to comment on the choice of the empirical relation of the type given by Eq. (4-1) for the estimation of the total contribution to the intensity from the overlap and quadrupolar components. When a functional relation represented by Eq. (3-1) was tried for the wings of these two types of components, no fit of the calculated profile to the experimental one could be obtained because of the

availability of the very few data points. Also the use of other empirical relations of exponential and power-law types for these wings was found to be of no avail. It is well-known that the dispersion line-shape decreases too slowly in the high wavenumber wing to represent experimental data satisfactorily. Finally, when the relation given by Eq.(4-1), which is basically a dispersion function with an extra term containing $\Delta\nu^4$ in the denominator, was used, a satisfactory fit was obtained. This function can be regarded as a truncated rational function expansion of the actual line-shape. The chosen parametrization makes Eq.(4-1) positive-definite. The choice of ν_s as the wavenumber of the $S_1(1) + S_0(1)$ transition which is the nearest strong transition, is only arbitrary and any other choice in that region would simply alter the values of the parameters a_1, a_2 and a_3 .

There are two very weak absorption features around 6000 and 6150 cm^{-1}, which have not been taken into account in this analysis. These wavenumber positions do not correspond to any U group of transitions. However, these absorption features may be due to the double transitions of the type $S_1(J) + S_0(J)$ involving J = 2 and 3 (because of high density of the gas), some of which fall in this region.

In the absorption profiles the U(0) group of transitions is completely masked by the strong $S_1(1) + S_0(1)$ transition. Experiments with pure para H_2 at 77 K may be performed to observe these transitions separately. Also investigation of pure rotational U transitions in the far infrared would be interesting.

APPENDIX 1

Matrix elements $\langle v'J'|\gamma|vJ\rangle$ of the anisotropy γ of the polarizability of H_2 in atomic units

(Poll, private communication)

v	J	v'	J'	$\langle v'J'\|\gamma\|vJ\rangle$
0	0	0	2	2.0351
0	1	0	3	2.0500
0	2	0	4	2.0725
0	3	0	5	2.1025
0	0	1	2	0.5708
0	1	1	3	0.5463
0	2	1	4	0.5232
0	3	1	5	0.5015

APPENDIX 2

Relative Intensities of the Overlap, Quadrupolar and Hexadecapolar transitions in the fundamental band of Hydrogen at 77 K. These are valid within the individual overlap, quadrupolar (due to isotropic polarizability), quadrupolar (due to anisotropy of polarizability) and hexadecapolar groups of transitions.

Transition	Wavenumber (cm^{-1})	Relative Intensity
Overlap Induction:		
	Transitions with J = 0 and 1	
$Q_1(1)$	4155.3	1.0000
$Q_1(0)$	4161.2	0.3311
	Transitions with J = 2 and 3	
$Q_1(3)$	4125.9	0.0000_4
$Q_1(2)$	4143.5	0.0022

Transition	Wavenumber (cm^{-1})	Relative Intensity
Quadrupolar Induction: (due to isotropic polarizability)		
	Transitions with J = 0 and 1	
$Q_1(1) + Q_0(J)$	4155.3	0.4232
$Q_1(1)$	4155.3	0.9942
$Q_1(0) + Q_0(J)$	4161.2	0.1398
$S_1(0)$	4497.8	0.6526
$Q_1(1) + S_0(0)$	4509.6	0.3506
$Q_1(0) + S_0(0)$	4515.6	0.1158
$S_1(1)$	4712.9	1.0000
$Q_1(1) + S_0(1)$	4742.3	0.6407
$Q_1(0) + S_0(1)$	4748.2	0.2116
	Transitions with J = 2	
$O_1(2)$	3806.8	-
$Q_1(2) + Q_0(J)$	4143.5	0.0009
$Q_1(2)$	4143.5	0.0015
$Q_1(2) + S_0(0)$	4497.8	0.0008
$Q_1(2) + S_0(1)$	4730.5	0.0014
$S_1(2)$	4917.0	0.0015
$Q_1(1) + S_0(2)$	4969.7	0.0012
$Q_1(0) + S_0(2)$	4975.6	0.0004

Transition	Wavenumber (cm^{-1})	Relative Intensity
Quadrupolar Induction: (due to the anisotropy of the polarizability)		
	Transitions with J = 0 and 1	
$S_1(0) + S_0(0)$	4852.2	0.3289
$S_1(1) + S_0(0)$	5067.3	0.5472
$S_1(0) + S_0(1)$	5084.9	0.6012
$S_1(1) + S_0(1)$	5299.9	1.0000
	Transitions with J = 2	
$S_1(2) + S_0(0)$	5271.4	0.0009
$S_1(0) + S_0(2)$	5312.2	0.0011
$S_1(2) + S_0(1)$	5504.0	0.0017
$S_1(1) + S_0(2)$	5527.3	0.0019
$S_1(2) + S_0(2)$	5731.4	0.00000_3
Hexadecapolar Induction		
	Transitions with J = 0 and 1	
$U_1(0)$	5271.4	0.6851
$Q_1(1) + U_0(0)$	5324.0	0.0782
$Q_1(0) + U_0(0)$	5330.0	0.0258
$U_1(1)$	5695.4	1.0000
$Q_1(1) + U_0(1)$	5776.9	0.1348
$Q_1(0) + U_0(1)$	5782.9	0.0445

APPENDIX 3

Program for Analysis of U-Transitions
on Hewlett Packard 9825A Calculator

```
0: wrt 6,"ANALYSIS OF U-TRANSITIONS; normal H2 at 77K"
1: "Pade Approximant Program;Uses Numerical Differentiation":
2: fmt 1,f8.1,3e18.8
3: fmt 2,10x,"A(",f2.0,")=",e20.8;fmt 3,"H,T are",2e16.8
4: fmt 9,"Wavenumber=",f7.2,"cm-1",3x,"Rel.Intensity=",f8.6
5: 5→X;.018685093→B;enp "# of U Transitions",S;dim O[S],I[S]
6: for J=1 to S;ent O[J],I[J];wrt 6.9,O[J],I[J];next J
7: enp "restart",T;if T#0;gto "restart"
8: ent Z;dim Y[Z],A[X],B[X],C[1,X],D[X,1],R[X],L[X,X],M[X,X],U[X,X]
9: rew;ert 0;mrk 1,40;mrk 1,10000
10: for J=1 to Z;ent Y[J];next J;rcf 0,Z;rcf 1,Y[*];gto "cont"
11: "restart":ldf 0,Z
12: dim Y[Z],A[X],B[X],C[1,X],D[X,1],R[X],L[X,X],M[X,X],U[X,X]
13: ldf 1,Y[*]
14: "cont":wrt 6,"Trial Values of A(J) are:"
15: wtb 6,10;for J=1 to X;ent A[J];wrt 6.2,J,A[J];next J;wtb 6,10
16: ent H,T;wrt 6.3,H,T
17: "BEGIN MAJOR ITERATION LOOP":for W=1 to 20
18: ina M,R;for K=1 to Z by 1;10K-10+5400→N
19: for J=1 to X
20: 'PADE'(N)→F
21: A[J](1+H)→A[J]
22: ('PADE'(N)-F)/A[J]H→D[J,1]
23: A[J]/(1+H)→A[J]
24: R[J]+D[J,1](Y[K]-F)→R[J]
25: next J
26: trn D→C;mat DC→L;ara L+M→H;next K
27: inv M→U;mat UR→B;ara A+B→A;aprt B
28: for J=1 to X;if abs(B[J]/A[J])<T;next J;gto "Break"
29: "END MAJOR ITERATION LOOP":dsp "Loop",W;next W
30: "...NONCONVERGENCE":wrt 6,"NONCONVERGENCE";wtb 6,7,7,7;stp
31: "Break":for K=1 to Z by 1;5400+10K-10→N
32: wrt 6.1,N,Y[K],'PADE'(N),Y[K]-'PADE'(N)
33: next K
34: wtb 6,10;wrt 6,"COMPUTED VALUES OF A(J) ARE:"
35: wtb 6,10;fmt 2,10x,"A(",f2.0,")=",e20.8
36: for J=1 to X;wrt 6.2,J,A[J];next J
37: wtb 6,10,10,7;dsp "END"; Calculates AREA";gto "Area"
38: "PADE":A[1]^2p1/(1+((p1-5300)/A[2])^2+((p1-5300)/A[5])^4)→r0
39: 0→r2;for L=1 to S
40: A[3]^2I[L]p1/(1+((p1-O[L])/A[4])^2)→r1
41: r1/(1+exp(-B(p1-O[L])))+r2→r2;next L;r2+r0→r0
42: ret r0
```

```
43: "QUAD":A[1]^2pl/(1+((pl-5300)/A[2])^2+((pl-5300)/A[5])^4)→r5
44: ret r5
45: "HEXA":A[3]^2I[pl]p2/(1+((p2-Q[pl])/A[4])^2)→r3
46: r3/(1+exp(-B(p2-Q[pl])))→r3
47: ret r3
48: "Area":
49: fmt 8,"Step Size=",f2.0,"cm-1",7x,"AREA of U1(1)=",e16.8,"cm-2"
50: for E=6400 to 7300 by 300;wrt 6,"Range=",E
51: for V=1 to 5;0→Y;4→J
52: for K=5400 to E by V;'HEXA'(J,K)+Y→Y;next K;YV2.3026/194.9→Y
53: wrt 6.8,V,Y;next V;next E;dsp "Plotter READY ?";stp
54: "Plot":scl 5400,5400+(Z-1)10,0,.5
55: axe 5400,0,50,.1
56: for K=1 to Z;plt 5400+10K-10,Y[K],-2;pen;next K
57: for K=1 to Z;plt 5400+10K-10,'PADE'(5400+10K-10),-2;next K;pen
58: for K=1 to Z;plt 5400+10K-10,'QUAD'(5400+10K-10),-2;next K;pen
59: for J=4 to S;for K=1 to Z
60: plt 5400+10K-10,'HEXA'(J,5400+10K-10),-2;next K;pen;next J
61: for K=1 to Z;0→r6;for J=1 to 3;'HEXA'(J,5400+10K-10)+r6→r6;next J
62: plt 5400+10K-10,r6;next K;pen
*8900
```

REFERENCES

Birnbaum, A. and Poll, J.D. 1969. J. Atmos. Sci. 26, 943.

Bosomworth, D.R. and Gush, H.P. 1965. Can. J. Phys. 43, 751.

Chang, K.S. 1974. Ph.D. Thesis, Memorial University of Newfoundland, St. John's, Newfoundland.

Chisholm, D.A. and Welsh, H.L. 1954. Can. J. Phys. 32, 291.

Crawford, M.F., Welsh, H.L. and Locke, J.L. 1949. Phys. Rev. 75, 1607.

Dean, J.W. 1961. National Bureau of Standards Technical Note 120 (U.S. Department of Commerce, Washington, D.C., U.S.A.).

Downie, A.R., Magoon, M.C., Purcell, T. and Crawford, Jr. B. 1953. J. Opt. Soc. Am. 43, 941.

Poltz, J.V., Rank, D.P. and Wiggins, T.A. 1966. J. Mol. Spectrosc. 21, 203.

Gibbs, P.W., Gray, C.G., Hunt, J.L., Reddy, S.P., Tipping, R.H. and Chang, K.S. 1974. Phys. Rev. Lett. 33, 256.

Goodwin, R.D., Diller, D.E., Rodes, H.M. and Weher, L.A. 1963. J. Res. Natl. Bur. Standards 67A, 173.

Humphreys, C.J. 1953. J. Opt. Soc. Amer. 43, 1027.

Hunt, J.L. and Welsh, H.L. 1964. Can. J. Phys. 42, 873.

IUPAC Tables of wavenumbers for calibration of Infrared Spectrometers, 1977. (Ed. A.R.H. Cole, Pergamon, Oxford-New York, 2nd Edition).

Karl, G., Poll, J.D. and Wolniewicz, L. 1975. Can. J. Phys. 53, 1781.

Kiss, Z.J. and Welsh, H.L. 1959. Can. J. Phys. 37, 1249.

Levine, H.B. and Birnbaum, G. 1967. Phys. Rev. 154, 86.

Lewis, J.C., 1976. Physica 82A, 500

Lewis, J.C. 1978. Private communication.

Mactaggart, J.W. and Welsh, H.L. 1973. Can. J. Phys. 51, 158.

McKellar, A.R.W. and Welsh, H.L. 1971. Proc. Roy. Soc. London, A 322, 421.

Plyler, E.K., Gailar, N.M. and Wiggins, T.A. 1952. J. Res. Natl. Bur. Standards. 48, 221.

Plyler, E.K., Blaine, L.R. and Tidwell, E.D. 1955. J. Res. Natl. Bur. Standards 55, 279.

Plyler, E.K., Danti, A., Blaine, L.R. and Tidwell, E.D. 1960. N.B.S. Monograph. no. 16.

Poll, J.D. 1960. Ph.D. Thesis, University of Toronto, Toronto, Ontario.

-------. 1971. Proc. I.A.U. Symposium No. 40 on planetary atmospheres, Marfa, Texas, October 1969 (Reidel Publications, Dordrecht, Holland).

-------. Private communication.

Poll, J.D. and Wolniewicz, L. 1978. J. Chem. Phys. 68, 3053.

Prasad, R.D.G. 1976. Ph.D. Thesis, Memorial University of Newfoundland, St. John's, Newfoundland.

Prasad, R.D.G., Clouter, M.J. and Reddy, S.P. 1978. Phys. Rev. A17, 1690.

Rao, K.N., Humphreys, C.J. and Rank, D.H. 1966. Wavelength Standards in the Infrared (Academic Press, New York).

Reddy, S.P., Varghese, G. and Prasad, R.D.G. 1977. Phys. Rev. A15, 975.

Reddy, S.P. and Kuo, C.Z. 1971. J. Mol. Spectrosc. 37, 327.

Van Kranendonk, J. 1957. Physica 23, 825.

-------. 1958. Physica 24, 347.

-------. 1968. Can. J. Phys. 46, 1173.

Van Kranendonk, J. and Kiss, Z.J., 1959. Can. J. Phys. 37, 1187.

Varghese, G., Ghosh, S.N. and Reddy, S.P. 1972. J. Mol. Spect. 41, 291.

Watanabe, A. 1971. Can. J. Phys. 49, 1320.

Watanabe, A. and Welsh, H.L. 1967. Can. J. Phys. 45, 2859.

Welsh, H.L. 1972. MTP International Review of Science, Physical Chemistry, Vol. 3, Spectroscopy (edited by D.A. Ramsay, Butterworths, London).

Welsh, H.L., Crawford, M.F. and Locke, J.L. 1949. Phys. Rev. 76, 580.

Zaidel', A.N., Prokofév, V.K., Raiskü, S.M., Slavnyi, V.A. and Shreider, E.Ya. 1970. Tables of spectral lines, (IFI|Plenum, New York-London).